

Disrupted antiferromagnetism in the brannerite MnV_2O_6

Simon A. J. Kimber and J. Paul Attfield

Centre for Science at Extreme Conditions, University of Edinburgh, Erskine Williamson Building, King's Buildings, Mayfield Road, Edinburgh EH9 3JZ, United Kingdom and School of Chemistry, University of Edinburgh, Joseph Black Building, King's Buildings, West Mains Road, Edinburgh EH9 3JJ, United Kingdom

(Received 27 November 2006; published 6 February 2007)

Magnetic order in brannerite type MnV_2O_6 has been studied by magnetization measurements and low temperature powder neutron diffraction. A sharp transition to a three-dimensionally ordered antiferromagnetic state is observed at $T_N=20$ K. Neutron diffraction at 5 K shows the spin structure to have a $(0\ 0\ 1/2)$ propagation vector with Mn^{2+} moments of $4.77(7)\ \mu_B$ ordered parallel to \mathbf{b} . Observed ferromagnetic order within chains of edge-sharing MnO_6 octahedra is consistent with a positive Weiss temperature of 5.8 K. The long range coherence of the magnetic order is limited, with a coherence length of 900 Å resulting from dilution of the Mn sites by 3% V due to intrinsic antisite disorder. The magnetic behavior of MnV_2O_6 is markedly different to that of the analogue CuV_2O_6 in which spin chain correlations were reported.

DOI: 10.1103/PhysRevB.75.064406

PACS number(s): 75.25.+z, 75.30.Et, 75.30.Cr, 75.50.Ee

I. INTRODUCTION

The ground states of low-dimensional magnetic systems are of continuing interest. Quantum ground states are particularly evident in spin 1/2 systems, for example, the one-dimensional materials CuGeO_3 (Ref. 1) and Sr_2CuO_3 (Ref. 2) which show a spin-Peierls transition and a spin gap, respectively, and the copper oxide superconductors which contain two-dimensional copper oxide planes.

Mixed oxides containing a magnetic and a nonmagnetic transition metal are a good source of low-dimensional crystal structures as $d^0\text{V}^{5+}$ in particular can adopt a range of coordinations. The structures of $M\text{V}_2\text{O}_6$ (monoclinic for $M=\text{Mn}$; triclinic for $M=\text{Co}, \text{Ni}, \text{Cu}$) are closely related to the brannerite (UTi_2O_6) structure³⁻⁵ and consist of chains of edge-sharing MO_6 octahedra parallel to the b axis connected by chains of corner and edge sharing VO_6 octahedra (Fig. 1). The magnetic properties of CuV_2O_6 have been widely investigated. Magnetization measurements showed a broad maximum at 44 K attributed to one-dimensional spin correlations in the CuO_6 chains, and long range antiferromagnetic order was confirmed at $T_N=24$ K by ESR.^{6,7} The intrachain and interchain exchange interactions were estimated to be $J_1/k=34$ K and $J_2/k=16.5$ K, respectively, by fitting an antiferromagnetic spin 1/2 Heisenberg chain model and CuV_2O_6 was also studied by powder neutron diffraction and ^{51}V and Cu NMR.⁸ The exchange interactions were further examined by spin dimer analysis using the extended Hückel method.⁹ Heat capacity measurements¹⁰ confirmed the onset of long range order in CuV_2O_6 to be 22.5 K and Zn doping experiments have shown rapid depression of long range antiferromagnetic order.¹¹ By contrast, the magnetic properties of the spin 5/2 analogue MnV_2O_6 or other $M\text{V}_2\text{O}_6$ brannerites have not been determined, although MnV_2O_6 has been studied as an electrode for lithium ion batteries.¹²⁻¹⁵ We report here the low temperature spin ordering in MnV_2O_6 determined from magnetization and neutron scattering measurements and the effects of an intrinsic Mn/V cation antisite disorder.

II. EXPERIMENT

Polycrystalline MnV_2O_6 was synthesised by a citrate gel decomposition technique. Stoichiometric quantities of manganese (II) acetate tetrahydrate (Aldrich, 99%+) and V_2O_5 (Aldrich, 99.99%) were dissolved in distilled water together with a threefold molar excess of acetic acid. The mixture was heated and stirred until a blue gel formed. The gel was allowed to solidify then decomposed at 300 °C for 3 h. The resulting solid was ground, pelleted, and heated at 600, 630, and 650 °C for 12, 12, and 72 h, respectively. The product was shown to be phase pure by powder x-ray diffraction. Magnetic susceptibility measurements were performed using a Quantum Design SQUID magnetometer in zero and field (1000 Oe) cooled conditions.

8 g of polycrystalline MnV_2O_6 were placed in a vanadium container and high resolution neutron diffraction patterns were recorded at 5 and 30 K using the instrument Super-D2B at the ILL, Grenoble, with a wavelength of $\lambda=1.594$ Å. The General Structures Analysis System (GSAS)¹⁶ was used to analyze the data by the Rietveld method.¹⁷

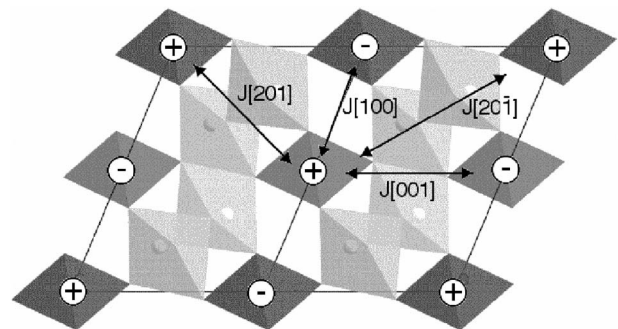


FIG. 1. Crystal and magnetic structure of MnV_2O_6 projected down $[010]$, dark octahedra are MnO_6 chains, light octahedra are VO_6 , + and - symbols represent up and down spins, respectively, schematic magnetic interaction pathways are also shown.

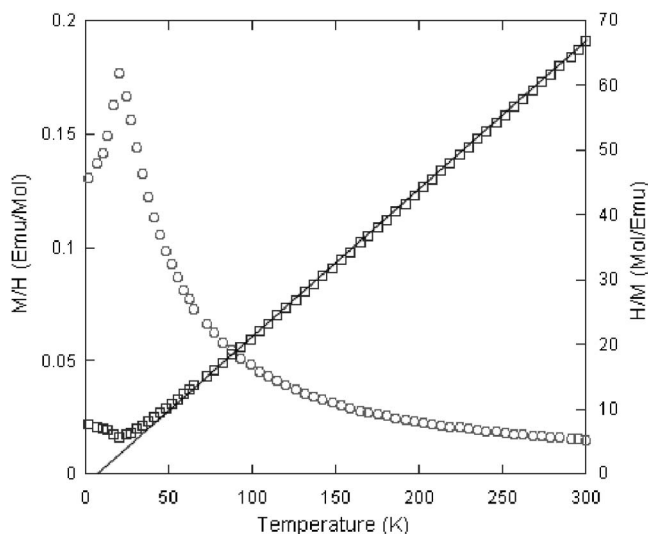


FIG. 2. Magnetic susceptibility of MnV_2O_6 and inverse susceptibility plotted as a function of temperature. Line shows Curie-Weiss fit to range 50–300 K extrapolated to low temperatures.

III. RESULTS

A. Magnetization measurements

The susceptibilities for MnV_2O_6 in Fig. 2 show a sharp transition to an antiferromagnetically ordered state below $T_N=20$ K, with no substantial low-dimensional correlations at higher temperatures. Above 50 K, the inverse susceptibility is fitted well by a Curie-Weiss law with a calculated moment of $5.96 \mu_B$, in good agreement with the expected spin only value for Mn^{2+} ($5.92 \mu_B$). No divergence between zero field and field cooled measurements was seen showing that no ferromagnetism or spin glass behavior occurs above 1.8 K. However, the Weiss temperature is positive (5.8 K), suggesting that significant ferromagnetic exchange interactions are present above T_N .

B. Neutron diffraction

No structural transitions are observed on cooling to 5 K. The 30 K neutron diffraction profile [Fig. 3(a)] was therefore fitted by refining the previously published room temperature structural model for MnV_2O_6 in space group $C2/m$.⁵ The peak shape was described by a pseudo-Voigt function with a correction for axial divergence¹⁸ and the background was modelled with a linear interpolation function. As Mn and V are both in octahedral coordination in the brannerite structure, the possibility of Mn/V antisite disorder was considered. The contrast between the neutron scattering lengths of Mn and V enabled their site occupancies to be refined precisely, under the constraint of preserving stoichiometry, and a small occupancy of 2.9(6)% V at the Mn sites was found. The refinement converged with residuals $wR_p=4.36\%$, $R_p=3.36\%$, and a goodness-of-fit $\chi^2=2.10$. The 30 K structure is similar to that reported previously at 300 K, with tetragonally compressed Mn^{2+} and distorted V^{5+} octahedra.

The neutron diffraction profile at 5 K [Fig. 3(b)] showed additional magnetic scattering peaks at low angles. These

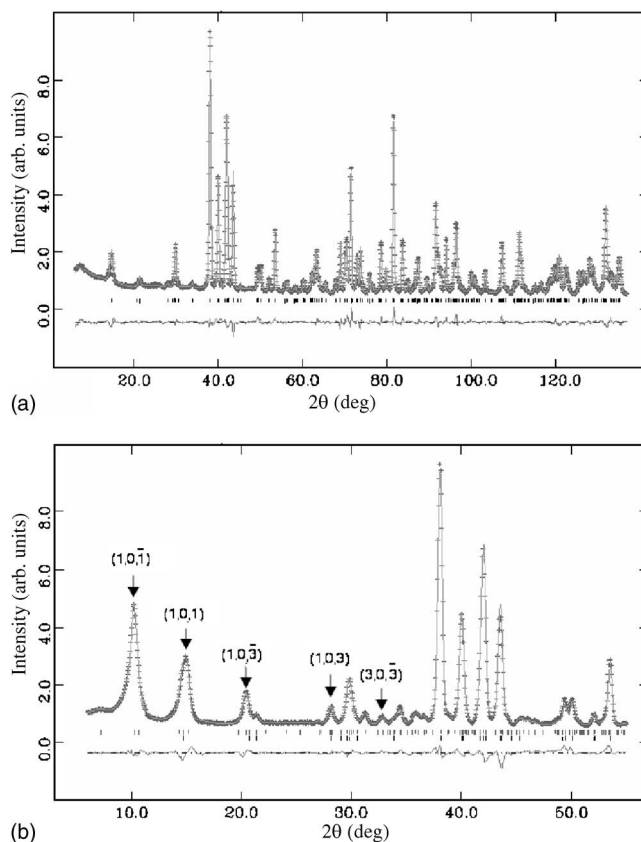


FIG. 3. Observed, calculated, and difference plots for the Rietveld fits to neutron diffraction profiles of MnV_2O_6 ; (a) refinement of the crystal structure at 30 K, (b) low angle region of the crystal and magnetic structure fit to the 5 K neutron data with prominent magnetic peaks labelled.

peaks belong to the class $(h\ 0\ l/2)$ with odd values of h and l , showing that the magnetic propagation vector is $(0,0,1/2)$. The magnetic intensities were fitted by an antiferromagnetic model (Fig. 1) in Shubnikov group P_c2/m , in which the Mn spins on $(0,0,0)$ are antiparallel to the spins on $(0.5,0.5,0)$ and $(0.5,0.5,0.5)$ and are aligned in the b direction. The refined magnitude of the Mn moment is $4.77(7) \mu_B$.

The 5 K magnetic diffraction peaks from MnV_2O_6 were observed to be significantly broader than the nuclear peaks, and so the Lorentzian peak-broadening coefficients Γ for the two sets of reflections were varied independently. The mean correlation length for the magnetic order ξ was estimated as $\xi=K\lambda/\Delta\Gamma$ where K is the Scherrer constant (0.9). The excess Lorentzian broadening $\Delta\Gamma$ was calculated as the difference between the Γ 's for the magnetic [3.09(4) rad] and nuclear [1.45(5) rad] reflections, assuming the latter to be limited by instrumental resolution. The estimated magnetic coherence length is thus $\xi\approx 900$ Å for MnV_2O_6 at 5 K. The fit of the magnetic model and the $C2/m$ nuclear structure to the 5 K neutron diffraction data is shown in Fig. 3(b). The residuals are $wR_p=5.25\%$, $R_p=4.03\%$, and $\chi^2=3.11$. Results of the 5 and 30 K refinements are summarized in Tables I and II.

TABLE I. Refined lattice parameters, atomic coordinates and thermal displacement parameters ($\text{\AA}^2 \times 10^2$) for MnV_2O_6 at 5 and 30 K. Atomic positions are Mn (0,0,0), V ($x, 0.5, z$), O(1) ($x, 0.5, z$), O(2) ($x, 0.5, z$), O(3) ($x, 0.5, z$). Metal site occupancies at 30 K are; Mn site 0.971(6) Mn/0.029 V, V site 0.015(3) Mn/0.985 V.

	5 K	30 K
a (\AA)	9.289(1)	9.289(1)
b (\AA)	3.5343(5)	3.5344(4)
c (\AA)	6.737(1)	6.738(1)
β ($^\circ$)	113.00(1)	112.96(1)
Volume (\AA^3)	203.61(4)	203.71(3)
Mn: Uiso	0.29(6)	0.11(5)
V: x	0.309(2)	0.316(2)
V: z	0.365(2)	0.359(2)
V: Uiso	0.29(6)	0.11(5)
O(1): x	0.1563(2)	0.1566(1)
O(1): z	0.1137(3)	0.1147(2)
O(1): Uiso	0.49(3)	0.54(3)
O(2): x	0.4684(1)	0.4683(1)
O(2): z	0.2902(2)	0.2894(2)
O(2): Uiso	0.48(3)	0.39(3)
O(3): x	0.1940(1)	0.1937(2)
O(3): z	0.5653(2)	0.5643(2)
O(3): Uiso	0.65(4)	0.44(4)

IV. DISCUSSION

The above results have shown that MnV_2O_6 undergoes a sharp Néel transition at $T_N=20$ K with no evidence for low-dimensional magnetism above this temperature. This is surprising in view of the crystal structure and the previously reported antiferromagnetic spin-chain behavior of the CuV_2O_6 analogue. The refined moment, 4.77(7) μ_B , is close to the expected value of 5 μ_B for Mn^{2+} , with a slight decrease due to covalency as is typical in insulating oxides, but without a large reduction that would indicate significant magnetic frustration.

The observed spin structure of MnV_2O_6 consists of ferromagnetic chains parallel to \mathbf{b} , with antiferromagnetic couplings to the nearest chains in the \mathbf{a} and \mathbf{c} directions, as shown in Fig. 1. Two possible magnetic structures were identified from a previous neutron diffraction study of CuV_2O_6 .⁸ Both models have ferromagnetic spin chains but they differ in the couplings between chains. Model A has antiferromagnetic coupling between chains along \mathbf{a} only leading to a propagation vector of (0,0,0), whereas the model B has antiferromagnetic couplings along \mathbf{a} and \mathbf{c} , giving a (0,0,1/2) vector. Extended Hückel calculations proposed that the strongest antiferromagnetic interaction is along \mathbf{c} , which favors model B for CuV_2O_6 .⁹ The spin arrangement we have determined for MnV_2O_6 is the same as the model B for CuV_2O_6 , suggesting that the differences between their short range orderings do not reflect different long range spin ordered ground states.

Although the long range order in MnV_2O_6 is antiferromagnetic, the positive Weiss temperature shows that signifi-

TABLE II. Selected interatomic distances (\AA) and angles ($^\circ$) for MnV_2O_6 at 5 K and 30 K.

	5 K	30 K
Mn-O(1) \times 4	2.225(5)	2.227(1)
Mn-O(2) \times 2	2.088(2)	2.083(1)
\langle Mn-O \rangle	2.179(2)	2.179(2)
Mn-O(1)-Mn	105.2(1)	105.0(1)
V-O(1) \times 1	1.74(2)	1.73(2)
V-O(2) \times 1	1.74(2)	1.66(2)
V-O(2) \times 1	2.43(2)	2.43(2)
V-O(3) \times 2	1.831(4)	1.853(4)
V-O(3) \times 1	2.02(2)	2.10(2)
\langle V-O \rangle	1.93(2)	1.94(2)
Mn-Mn: $\perp b$	4.9695(1)	4.96969(6)
	6.737(1)	6.738(1)
Mn-Mn: $\parallel b$	3.53430(5)	3.53448(5)

cant ferromagnetic interactions are present. This is consistent with the observed parallel alignment of Mn^{2+} spins within the chains of edge-sharing MnO_6 octahedra. Ferromagnetism within such chains is unusual, although $\text{YCa}_3(\text{MnO})_3(\text{BO}_3)_4$, which also contains chains of edge-sharing Mn^{2+}O_6 octahedra, has a positive Weiss temperature of $\theta=27$ K.¹⁹ Dominant antiferromagnetic direct exchange from e_g - e_g orbital interactions would be expected,²⁰ but this may be outweighed by ferromagnetic t_{2g} - t_{2g} superexchange through the Mn-O-Mn bridges.²¹ In contrast, the intrachain exchange interaction in CuV_2O_6 is unexpectedly weak due to orbital ordering as the unpaired electron resides in the $d_{x^2-y^2}$ type orbital so there is little interaction between nearest neighbor Cu^{2+} spins. A schematic representation of the interchain exchange interactions in MnV_2O_6 is shown in Fig. 1. Each chain is coupled antiferromagnetically to the two nearest neighbors via the $J[001]$ and $J[100]$ interactions through the VO_6 octahedra,²² with only the weaker $J[201]$ and $J[20\bar{1}]$ interactions frustrated.

Although the magnetic order in MnV_2O_6 appears almost unfrustrated in the ideal structure, the Scherrer broadening of the magnetic diffraction peaks shows that the long range order is frequently disrupted as it is coherent only over ~ 900 \AA (~ 150 mean lattice repeats) at 5 K. The related material CoNb_2O_6 , which has a similar structure type, has strongly anisotropic magnetic coherence lengths because of competition between the interchain exchange interactions and single ion anisotropy.²³ No (hkl) dependence of the broadening is evident for MnV_2O_6 and we speculate that the origin of the reduced correlation length in MnV_2O_6 is the 3% Mn/V antisite disorder. We note that this ‘‘self-diluting’’ effect may be present in other stoichiometric MV_2O_6 brannerites to a greater extent, as the M/V size disparity decreases as M changes from Mn to Cu. This disruption could contribute to the suppression of long range order in CuV_2O_6 , as diamagnetic doping usually has a pronounced effect on low-dimensional magnetic materials.

In summary, MnV_2O_6 is found to behave as a three-dimensional antiferromagnet with a Néel transition at 20 K.

The observed ordered magnetic moment is consistent with unfrustrated order of Mn^{2+} $S=5/2$ spins. The magnetic structure has a $(0,0,1/2)$ propagation vector, and corresponds to one of the two models previously proposed for CuV_2O_6 . No evidence for substantial short range correlations is observed in MnV_2O_6 , in contrast to CuV_2O_6 which shows low-dimensional antiferromagnetic correlations. This is likely due to the different balance of exchange interactions because of orbital ordering of Cu^{2+} or the greater contribution of quantum effects for $S=1/2$ spins. The coherence length for spin order in MnV_2O_6 is only ~ 900 Å because of

intrinsic Mn/V antisite disorder within this stoichiometric material.

ACKNOWLEDGMENTS

The authors thank the EPSRC for provision of beam time at the ILL and a studentship for S.A.J.K, and the Leverhulme Trust for support. We also thank G.B.S. Penny (UoE), L. Ortega (UoE) and A.W. Hewat (ILL) for assistance with the neutron measurements.

-
- ¹M. Hase, I. Terasaki, and K. Uchinokura, *Phys. Rev. Lett.* **70**, 3651 (1993).
²N. Motoyama, H. Eisaki, and S. Uchida, *Phys. Rev. Lett.* **76**, 3212 (1996).
³J. Ziolkowski, K. Krupa, and M. Mocala, *J. Solid State Chem.* **48**, 376 (1983).
⁴K. Mocala and J. Ziolkowski, *J. Solid State Chem.* **69**, 299 (1987).
⁵H. K. Müeller-Buschbaum and M. Kobel, *J. Alloys Compd.* **176**, 39 (1991).
⁶A. N. Vasil'ev, L. A. Ponomarenko, A. I. Smirnov, E. V. Antipov, Y. A. Velikodny, M. Isobe, and Y. Ueda, *Phys. Rev. B* **60**, 3021 (1999).
⁷A. N. Vasil'ev, L. A. Ponomarenko, E. V. Antipov, Y. A. Velikodny, A. I. Smirnov, M. Isobe, and Y. Ueda, *Physica B* **284**, 1615 (2000).
⁸J. Kikuchi, K. Ishiguchi, K. Motoya, M. Itoh, K. Inari, N. Eguchi, and J. Akimitsu, *J. Phys. Soc. Jpn.* **69**, 2660 (2000).
⁹H.-J. Koo and M.-H. Whangbo, *J. Solid State Chem.* **156**, 110 (2001).
¹⁰A. V. Prokofiev, R. K. Kremer, and W. Assmus, *J. Cryst. Growth* **231**, 498 (2001).
¹¹M. Belaïche, M. Bakhache, M. Drillon, and A. Derory, *Chem. Phys. Lett.* **394**, 147 (2004).
¹²D. Hara, H. Ikuta, Y. Uchimoto, and M. Wakihara, *J. Mater. Chem.* **12**, 2507 (2002).
¹³D. Hara, H. Ikuta, Y. Uchimoto, M. Wakihara, T. Miyanaga, and I. Watanabe, *J. Mater. Chem.* **12**, 3717 (2002).
¹⁴M. Inagaki, T. Morishita, M. Hirano, V. Gupta, and T. Nakajima, *Solid State Ionics* **156**, 275 (2003).
¹⁵T. Morishita, K. Nomura, T. Inamasu, and M. Inagaki, *Solid State Ionics* **176**, 2235 (2005).
¹⁶A. C. Larson and R. B. Von Dreele, Los Alamos National Laboratory Report No. LAUR 86-748 (1994) (unpublished).
¹⁷H. M. Rietveld, *J. Appl. Crystallogr.* **2**, 65 (1969).
¹⁸L. W. Finger, D. E. Cox, and A. P. Jephcoat, *J. Appl. Crystallogr.* **27**, 892 (1994).
¹⁹R. K. Li and C. Greaves, *Phys. Rev. B* **68**, 172403 (2003).
²⁰J. B. Goodenough, *Phys. Rev.* **117**, 1442 (1960).
²¹J. B. Goodenough, *Magnetism and the Chemical Bond* (Interscience, New York, 1963).
²²J. M. Mays, *Phys. Rev.* **131**, 38 (1963).
²³S. Kobayashi, S. Mitsuda, K. Hosoya, H. Yoshizawa, T. Hanawa, M. Ishikawa, K. Miyatani, K. Saito, and K. Kohn, *Physica B* **213**, 176 (1995).